Very low threshold operation of quantum cascade lasers*

Yan Fang-Liang(闫方亮), Zhang Jin-Chuan(张锦川)†, Yao Dan-Yang(姚丹阳), Liu Feng-Qi(刘峰奇)‡, Wang Li-Jun(王利军), Liu Jun-Qi(刘峻岐), and Wang Zhan-Guo(王占国)

Key Laboratory of Semiconductor Materials Science, Institute of Semiconductors, Chinese Academy of Sciences, and Beijing Key Laboratory of Low Dimensional Semiconductor Materials and Devices, Beijing 100083, *China*

(Received 19 May 2014; revised manuscript received 22 August 2014; published online 10 December 2014)

A strain-compensated InP-based quantum cascade laser (QCL) structure emitting at 4.6 μm is demonstrated, based on a two-phonon resonant design and grown by solid-source molecular beam epitaxy (MBE). By optimizing the growth parameters, a very high quality heterostructure with the lowest threshold current densities ever reported for QCLs was fabricated. Threshold current densities as low as 0.47 kA/cm^2 in pulsed operation and 0.56 kA/cm^2 in continuous-wave (cw) operation at 293 K were achieved for this state-of-the-art QCL. A minimum power consumption of 3.65 W was measured for the QCL, uncooled, with a high-reflectivity (HR) coating on its rear facet.

Keywords: semiconductor laser, quantum cascade lasers, threshold current density

PACS: 42.55.PX, 85.35.Be **DOI:** 10.1088/1674-1056/24/2/024212

1. Introduction

Quantum cascade lasers (QCLs) have been proven in the past 20 years to be ideal infrared sources.[1,2] High quality materials are among the key requirements for realizing high-performance quantum cascade lasers. Given stable and flexible control of emission wavelength, QCLs provide efficient and versatile sources for chemical sensing applications in the mid-infrared range.[3] Continuous-wave (cw) operation at room temperature,[4–7] high power,[8] and single mode operation[9] have been demonstrated in systems fabricated from several different materials,[10–12] spanning the infrared spectral range. The performance of QCLs has been improved significantly since the first QCL was demonstrated,[13] with wall-plug efficiency (WPE) exceeding 20% and optical power of 5 W in cw mode at room temperature.[14]

However, efficiency remains a concern because the cooling subsystem is typically larger and more power-hungry than the laser itself. Therefore, among all of the device parameters, lower threshold current density is specially demanded in order to reduce the system's electricity consumption and achieve higher WPE. With recent progress in materials growth, device fabrication and active-region design, the threshold current density of QCL has been significantly reduced to around 1 kA/cm^2 at room temperature.[6,7,14–16] In this letter, we report a further reduction of the threshold current densities to unprecedented values. The threshold current densities are as low as 0.47 kA/cm^2 in pulsed operation and 0.56 kA/cm^2 in cw operation at 293 K.

2. Device fabrication

The QCL structure was grown on an n-doped (Si, 2×10^{17} cm^{-3}) InP substrate by solid-source molecular beam epitaxy (MBE). The laser's active region consists of 30 stages that are designed to emit at a wavelength of 4.6 μm. In order to minimize the losses that are due to optical mode leakage into the substrate, a 1.2-μm InP lower cladding (Si, 2.2×10^{16} cm^{-3}) was first grown on the wafer. The average doping level was adjusted to 2.4×10^{16} cm^{-3} toward the core of the structure to reduce the free-carrier absorption that is due to the overlap of the optical mode with highly doped regions. In order to concentrate the optical mode in the center of the structure, a standard waveguide was employed, consisting of a 2.4-μm InP upper cladding layer (Si, 2.2×10^{16} cm^{-3}) and a 0.6-μm InP cap cladding layer (Si, 1×10^{19} cm^{-3}). The entire waveguide structure is identical to that described in Ref. [17].

The QCL active region is based on the two-phonon resonant design presented in Ref. [18]. The active region is designed to obtain both high injection efficiency from the ground level of the injector to the upper laser level and a short lifetime (0.2 ps∼0.4 ps) of the lower lasing state.[19] At short wavelengths, in order to prevent thermal escape of the carrier, a material system with a large conduction band discontinuity is required. Therefore, we used highly strained (∼1%) $In_{0.669}Ga_{0.331}As$ quantum wells and $In_{0.362}Al_{0.638}As$ barriers, which are totally strain-compensated in each stage. This provides a barrier height that is considerably larger (823 meV instead of 520 meV) than that found in unstrained materials. As a result, electron tunneling from the upper laser states into the continuum can be efficiently reduced.[20,21] Addition-

*Project supported by the National Basic Research Program of China (Grant Nos. 2013CB632801 and 2013CB632803), the National Natural Science Foundation of China (Grant Nos. 61306058, 61274094, and 61435014), and the Beijing Natural Science Foundation (Grant No. 4144086).

†Corresponding author. E-mail: zhangjinchuan@semi.ac.cn

‡Corresponding author. E-mail: fqliu@semi.ac.cn

© 2015 Chinese Physical Society and IOP Publishing Ltd

ally, control of laser materials and interface quality are key issues in improving device performance. To this end, extensive work has been done and optimal growth parameters have been adopted.[4,22] We used a solid-source MBE system with valved crackers for arsenic and phosphorus, and dual filament effusion cells for Ga, Al, and In sources. The quality of the grown material is very sensitive to the substrate temperature. Considering that $In_{0.362}Al_{0.638}As$ tends to have a better crystallization quality at high substrate temperature (520 °C∼550 °C) and $In_{0.669}Ga_{0.331}As$ has a better crystallization quality at low substrate temperature (460 °C∼510 °C), we used an intermediate substrate temperature of 510 °C during the growth of the laser core. The temperature stability was calibrated to better than 0.3 °C during the growth of the entire structure. In order to improve the surface roughness of the $In_{0.362}Al_{0.638}As$ and $In_{0.669}Ga_{0.331}As$ layers, an optimum V/III flux ratio (the incident flux ratio between As and Ga, In, or Al) was chosen at 17∼19, which is higher than usual. The optimum growth rate of 0.7 μm/h∼0.9 μm/h was chosen by considering both the crystallization and growth time. The use of solid-source MBE may be advantageous for improving the interface quality, in contrast to gas-source MBE or metal organic vapor-phase epitaxy (MOVPE). Therefore, we observed no detrimental effects, like the broadening of the electroluminescence (EL) spectrum, arising from the use of strain-compensated material. Typical x-ray diffraction curves of the QCL structure are shown in Fig. 1(a). Excellent material quality and uniformity are observed, with a very narrow (11 arcsec–13 arcsec) full width at half maximum (FWHM) measurements of the satellite peaks. The zeroth peak is almost perfectly matched to the InP substrate peak, indicating that the strain-compensated active region layers do indeed provide a net zero strain. The larger proportion of Indium in the quantum wells results in a low effective mass of the electrons. Therefore, thicker wells can be designed, which has a positive effect on the interface quality.[18] The high quality of interfaces is confirmed by EL measurements, with a narrow FWHM of ∼17.4 meV at room temperature, as shown in Fig. 1(b). The narrow linewidth indicates that the heterojunction interface is sharp in the QCL structure.[23]

The epi-wafer was etched into double-channel geometry with a ridge width of 12 μm. A narrow active core can also decrease the total amount of strain that builds up in a material. A 450-nm-thick SiO_2 layer was deposited by chemical vapor deposition for electrical insulation. The SiO_2 layer was then removed by wet chemical etching from the top of the ridges, and electrical contacts were made by a Ti/Au layer deposition. An additional 5-μm-thick gold layer was electroplated to further improve heat dissipation. The laser was cleaved into 4-mm-long bars. Testing was performed on HR-coated cavities. An HR coating, consisting of Al_2O_3/Ti/Au/Al_2O_3 (200/10/100/120 nm), was deposited on the back facet by e-beam evaporation. The lasers were mounted epilayer-side down on diamond heat sinks with indium solder for effective heat dissipation. The lasers were then wire bonded and mounted on a holder containing a thermistor to monitor the heat sink temperature. A thermistor was mounted ∼2.5 mm away from the laser chip on a diamond submount for temperature monitoring. The optical power emitted from the uncoated facet of the laser was measured with a calibrated thermopile detector that was placed directly in front of the laser facet.

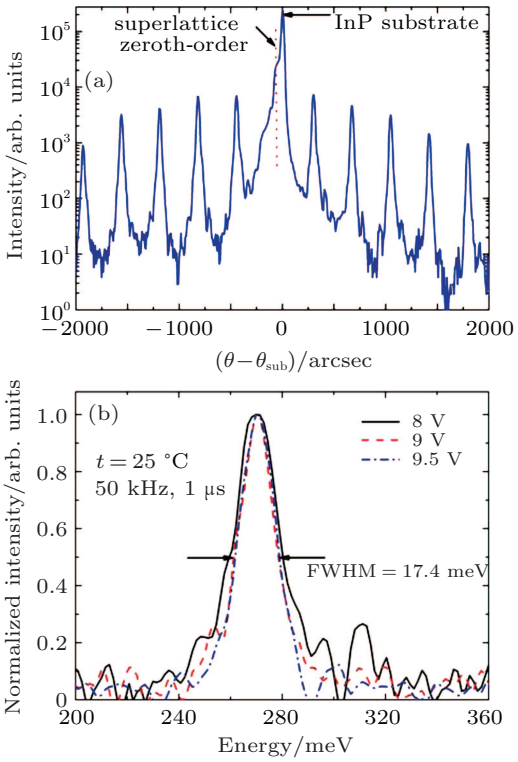


Fig. 1. (color online) (a) The x-ray diffraction spectrum of the QCL wafers; (b) measurement of the electroluminescence spectrum (EL) pumped with a 1-μs pulse and 50-kHz repetition frequency at 25 °C.

3. Laser characterization

Figure 2 shows the electrical and optical characteristics curves for different temperatures between 20 °C and 50 °C. To minimize the heating of the samples, the lasers were measured using 800-ns long pulses at a repetition rate of 10 kHz. A peak optical power of 560 mW was obtained at 20 °C with a threshold current density (J_{th}) of 0.47 kA/cm^2 and slope efficiency of 1.645 W/A. A peak power of 380 mW with a threshold current density (J_{th}) of 0.58 kA/cm^2 and slope efficiency of 1466 mW/A was measured at 50 °C. A characteristic temperature (T_0) of 167 K was calculated with $J_0 = 0.07$ kA/cm^2(inset of Fig. 2). We also calculated the waveguide loss by the comparing threshold currents between an HR-coated laser and uncoated laser, using the equation $J_{th} = (\alpha_w + \alpha_m)/g\Gamma$ where α_w is the waveguide loss, $\alpha_m = (1/2L)\ln(1/R_1R_2)$ the mirror loss, Γ the optical confinement factor and g the normal-

ized gain coefficient. The threshold currents of the HR-coated laser and the uncoated laser, both operating in pulsed mode at 20 °C, are 0.23 A and 0.35 A, respectively. The α_m values of the HR-coated laser and the uncoated laser are 1.65 cm^{-1} and 3.23 cm^{-1}, respectively, assuming reflectivity of 27.4% for uncoated facets and 95% for HR-coated facets. Thus, the calculated waveguide loss is 1.35 cm^{-1}. The modal gain coefficient Γg was deduced to be 6.38 cm/kA.

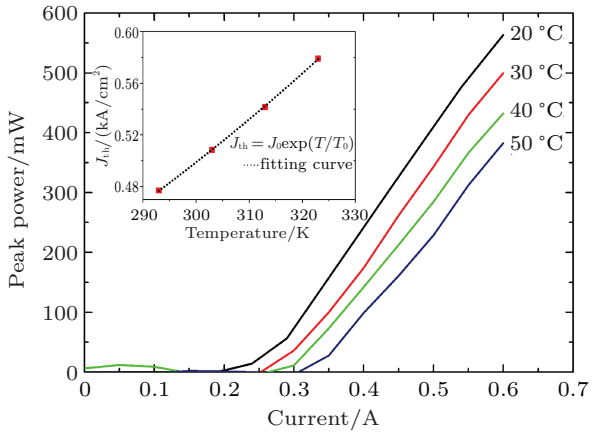


Fig. 2. (color online) Peak power versus current of the QCL operated in pulsed mode at different heat sink temperatures between 20 °C and 50 °C. Inset shows the temperature dependence of the threshold. The dotted line denotes an exponential fit to the experimental data.

Figure 3 shows the cw operated power–current–voltage (P–I–V) characteristics recorded between 20 °C and 60 °C. To avoid damage the lasers were not tested to their maximum operating temperature in this configuration. Maximum cw output powers of 402 mW and 203 mW were obtained at 20 °C and 60 °C, respectively. At 20 °C, cw threshold current density (J_{th}) as low as 0.56 kA/cm^2 was measured, which is lower than all of the previously reported values. The cw threshold power consumption is only 2.83 W at 20 °C corresponding to a high slope efficiency of 1.266 W/A. Even at a temperature of 60 °C, a threshold current density of 0.85 kA/cm^2 and slope efficiency of 987 mW/A are measured. The high optical power and low threshold characteristics are due mainly to the superior material quality, especially interface quality, that we obtained by employing a solid-source MBE.

A number of applications, such as free space optical communication, military countermeasures, mid-infrared pointers, need QCL with reduced electric power consumption and simple thermal management. Therefore, uncooled operation[17,24] (with no active cooling) is also a common requirement for QCL chips operated in cw mode at room temperature. In the present work, we have achieved lower electric power consumption than has been previously reported. Figure 4 shows the uncooled cw operation P–I–V characteristics of this QCL device at a nominal temperature of 290 K. The maximum cw output power is 300 mW, with a low threshold current density of 0.67 kA/cm^2. At saturation power, the injection current density is only 1.35 kA/cm^2. For uncooled cw operation, the electrical power consumption at the threshold is 3.65 W and the input electrical power is only 8.39 W at maximum optical output power. These are, to date, the lowest threshold current density and electrical power consumption figures reported for uncooled QCLs emitting at 4.6 μm. The inset of Fig. 4 gives the heat sink temperature increase as a function of injection electrical power. We observe a nearly linear correlation between heat sink temperature and injection electrical power. The heat sink temperature for an uncooled device operating at 290 K is measured to be only 310 K at maximum output power. For the device reported here, the additional thermal resistance $R_{th} = 2.18$ K/W is deduced from the inset of Fig. 4.[25] In the future, careful thermal packaging of such a device should further improve the uncooled cw performance with respect to low power consumption, high cw output power and high WPE operation.

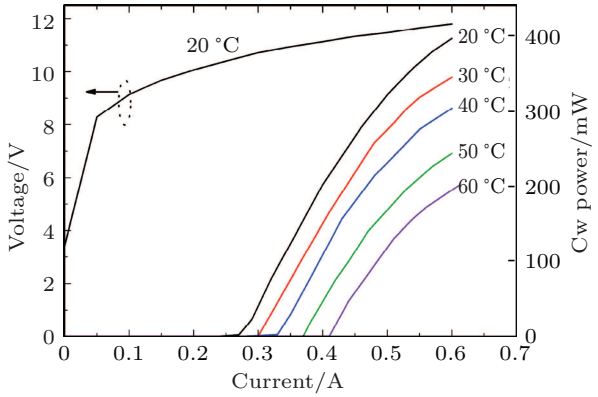


Fig. 3. (color online) The cw power–current–voltage characteristics of the QCL operated in cw mode at different heat sink temperatures between 20 °C and 60 °C along with V–I curves at 20 °C.

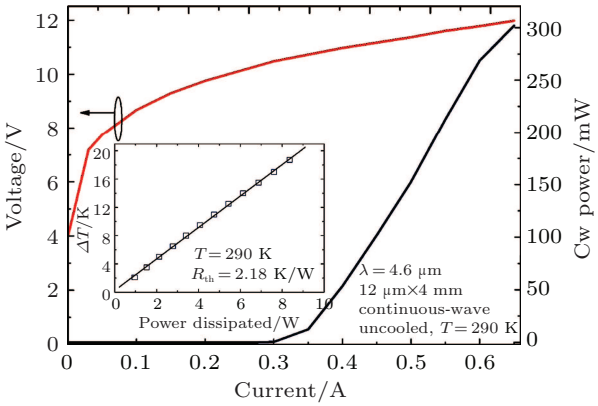


Fig. 4. (color online) The cw power–current–voltage characteristic of an uncooled cw QCL. Inset shows the heat sink temperature as a function of injection electrical power.

4. Conclusion

In conclusion, a high performance QCL structure grown by solid-source MBE was demonstrated with a very low threshold in cw mode at room temperature. These results show the potential of this MBE system for the growth of high quality

materials. By optimizing the growth parameters, we reduced the room-temperature threshold current density of this QCL to unprecedented values. Threshold current densities as low as 0.47 kA/cm^2 in pulsed operation and 0.56 kA/cm^2 in cw operation at 293 K were achieved for this HR-coated QCL. Uncooled operation of the QCL was obtained with a power consumption of only 3.65 W at the threshold and a threshold current density of 0.67 kA/cm^2. For further improvement, buried ridge QCL devices are in development to further reduce the power consumption and the threshold current density.

Acknowledgments

We acknowledge the contributions of Liang Ping and Hu Ying in the device fabrication.

References

[1] Kosterev A A and Tittel F K 2002 *IEEE J. Quantum Electron.* **38** 582
[2] Nelson D D, Shorter J H, McManus J B and Zahniser M S 2002 *Appl. Phys. B: Lasers Opt.* **75** 343
[3] Namjou K, Cai S, Whittaker E A, Faist J, Gmachl C, Capasso F, Sivco D L and Cho A Y 1998 *Opt. Lett.* **23** 219
[4] Liu F Q, Li L, Wang L J, Liu J Q, Zhang W, Zhang Q D, Liu W F, Lu Q Y and Wang Z G 2009 *Appl. Phys. A* **97** 527
[5] Xie f, Caneau C G, LeBlanc H P, Visovsky N J, Coleman S, Hughes L C and Zah C 2009 *Appl. Phys Lett.* **95** 091110
[6] Lyakh A, Maulini R, Tsekoun A, Go R, Pflügl C, Diehl L, Wang Q J, Capasso F and Patel C K N 2009 *Appl. Phys. Lett.* **95** 141113
[7] Wittmann A, Bonetti Y, Fischer M, Faist J, Blaser S and Gini E 2009 *IEEE Photon. Technol. Lett.* **21** 12
[8] Bai Y, Slivken S, Darvish S R, Haddadi A and Gokden B 2009 *Appl. Phys. Lett.* **95** 221104
[9] Lu Q Y, Guo W H, Zhang W, Wang L J, Liu J Q, Li L, Liu F Q and Wang Z G 2010 *Appl. Phys. Lett.* **96** 051112
[10] Sirtori C, Faist J, Capasso F, Sivco D L, Hutchinson A L, George Chu S N and Cho A Y 1996 *Appl. Phys. Lett.* **68** 1745
[11] Pflugl C, SchrenkW, Anders S, Strasser G, Becker C, Sirtori C, Bonetti Y and Muller A 2003 *Appl. Phys. Lett.* **83** 4698
[12] Cathabard O, Teissier R, Devenson J, Moreno J C and Baranov A N 2010 *Appl. Phys. Lett.* **96** 141110
[13] Faist J, Capasso F, Sivco D L, Sirtori C, Hutchinson A L and Cho A Y 1994 *Science* **264** 553
[14] Bai Y, Bandyopadhyay N, Tsao S, Slivken S and Razeghi M 2011 *Appl. Phys. Lett.* **98** 181102
[15] Wang X J, Fan J Y, Tanbun-Ek T and Choa F S 2007 *Appl. Phys. Lett.* **90** 211103
[16] Zhang J C, Wang L J, Chen J Y, Zhao L H, Liu F Q, Liu J Q, Li L and Wang Z G 2011 *Electron. Lett.* **47** 1338
[17] Zhang J C, Liu F Q, Tan S, Yao D Y, Wang L J, Liu J Q, Li L and Wang Z G 2012 *Appl. Phys. Lett.* **100** 112105
[18] Faist J, Hofstetter D, Beck M, Aellen T, Rochat M and Blaser S 2002 *IEEE J. Quantum Electron.* **38** 533
[19] Hofstetter D, Beck M, Aellen T and Faist J 2001 *Appl. Phys. Lett.* **78** 396
[20] Liu F Q, Zhang Y Z, Zhang Q S, Ding D, Xu B and Wang Z G 2000 *Semicond. Sci. Technol.* **15** L44
[21] Yu J S, Evans A, Slivken S, Darvish S R and Razeghi M 2006 *Appl. Phys. Lett.* **88** 251118
[22] Zhang J C, Liu F Q, Wang L J, Chen J Y, Zhai S Q, Liu J Q and Wang Z G 2013 *IEEE Photon. Technol. Lett.* **25** 686
[23] Tsujino S, Borak A, Müller E, Scheinert M, Falub C V, Sigg H, Grützmacher D, Giovannini M and Faist J 2005 *Appl. Phys. Lett.* **86** 062113
[24] Maulini R, Lyakh A, Tsekoun A, Go R, Pflügl C, Diehl L, Capasso F and Patel C K N 2009 *Appl. Phys. Lett.* **95** 151112
[25] Maulini R, Lyakh A, Tsekoun A, Go R and Patel C K N 2011 *Electron. Lett.* **47** 395